Daunomycin Intercalation Stabilizes Distinct Backbone Conformations of DNA

http://www.jbsdonline.com

Michael Trieb
Christine Rauch
Bernd Wellenzohn
Fajar Wibowo
Thomas Loerting
Erwin Mayer
Klaus R. Liedl*

Institute of General

Inorganic and Theoretical Chemistry

University of Innsbruck

Innrain 52a

A-6020 Innsbruck

Austria

Abstract

Daunomycin is a widely used antibiotic of the anthracycline family. In the present study we reveal the structural properties and important intercalator-DNA interactions by means of molecular dynamics. As most of the X-ray structures of DNA-daunomycin intercalated complexes are short hexamers or octamers of DNA with two drug molecules per doublehelix we calculated a self complementary 14-mer oligodeoxyribonucleotide duplex d(CGCGCGATCGCGCG)$_2$ in the B-form with two putative intercalation sites at the 5′-CGA-3′ step on both strands. Consequently we are able to look at the structure of a 1:1 complex and exclude crystal packing effects normally encountered in most of the X-ray crystallographic studies conducted so far. We performed different 10 to 20 ns long molecular dynamics simulations of the uncomplexed DNA structure, the DNA-daunomycin complex and a 1:2 complex of DNA-daunomycin where the two intercalator molecules are stacked into the two opposing 5′-CGA-3′ steps. Thereby – in contrast to X-ray structures – a comparison of a complex of only one with a complex of two intercalators per doublehelix is possible. The chromophore of daunomycin is intercalated between the 5′-CG-3′ bases while the daunosamine sugar moiety is placed in the minor groove. We observe a flexibility of the dihedral angle at the glycosidic bond, leading to three different positions of the ammonium group responsible for important contacts in the minor groove. Furthermore a distinct pattern of B$_I$ and B$_{II}$ around the intercalation site is induced and stabilized. This indicates a transfer of changes in the DNA geometry caused by intercalation to the DNA backbone.

Introduction

Daunomycin is of great importance as an anticancer drug. It is among the most potent and clinically useful agents currently used in cancer chemotherapy (1). A wealth of studies was performed to understand the structural, kinetic and energetical contributions of drug intercalation (2-16). In order to improve the sequence specificity of intercalators, bisintercalators and hybrid ligands were developed (17-23). For the structure based design of new ligands the knowledge of the exact conformational behavior is necessary. High resolution X-ray (24-29) and NMR (30) analyses have shown that intercalation often involves changes of sugar puckering and modifies the groove width. Furthermore a water uptake was found to accompany the complexation with daunomycin (31). Daunomycin is a naturally occurring anti-tumor antibiotic from a fungus belonging to the Streptomyces family. It is a member of the anthracycline family and consists of a planar aromatic ring system, a fused cyclohexane ring and an amino sugar moiety. Emerging from daunomycin some thousand new anthracycline analogs were synthesized in the search for a stronger biological activity and a lower toxicity. Molecular dynamics simulations haven proven their ability to predict the structure and dynamics of DNA and its interactions with ligands (32-43). In this paper we describe details of the three dimensional structure of daunomycin bound to the oligonucleotide duplex d(CGCGCGATCGCGCG)$_2$ in the B-form as determined by molecular modelling. Several mechanisms for the intercalation process in vivo have in common that the

1

Trieb et al.

biological activity of daunomycin supposedly results from intercalation of the chromophore structure into DNA and thereby changing DNA inherent parameters. The site selectivity for daunomycin has been investigated thoroughly giving different results depending on the methods and circumstances chosen but clearly has a preference for purine-pyrimidine in common (11, 44-46). As found by Frederick *et al.* (26) it shows a preference for 5´-CGA-3´ steps in B-form DNA. Furthermore molecular modelling studies which only apply minimization, no dynamics and treat only one layer of water molecules have proposed that the sugar part interacts with three successive base pairs being important for sequence recognition (47). An important advantage of our approach is the fact that we use explicit solvent unlike in X-ray structures where only a reduced number of crystal waters can be found. As far as we know there are only crystal structures of short DNA double strands comprising mostly of six base pairs with two daunomycins per DNA molecule intercalated between the last base pairs. However, binding studies investigating the kinetics and site selectivity of daunomycin with longer stretches of DNA, for example calf thymus DNA (3, 4, 48) and 16-mers (45), were conducted. Another recent study treats the free energy differences of anthracycline binding and ascribes different contributions of functional groups to the free energy (12). In these investigations a control of mono or double intercalation is hard to achieve if not impossible. By means of molecular modelling we are able to construct a longer strand of DNA and pose one single intercalator into a preferred site, and thereby circumventing the limitations of double intercalation and side effects. Our special interest lies in the change of stacking interactions at the site of intercalation as well as in the change of groove width. Another topic was the backbone conformation in terms of B_I/B_{II}. Their existence was first suggested (49) and then shown by X-ray crystallography (50, 51). The two substates B_I and B_{II} are defined by different conformations of the sugar phosphate backbone (52). The changes are characterized with the ε and ζ angles of the DNA backbone or by the angle difference ($\varepsilon - \zeta$). In the B_I state the corresponding ε and ζ angles are between 120º and 210º (trans) and between 235º and 295º (gauche-), respectively. For B_{II}, the ε angle lies between 210º and 300º (gauche-), and ζ lies between 150º and 210º (trans). The angle difference ($\varepsilon - \zeta$) is close to -90º for B_I and +90º for B_{II} phosphates (53-62). The investigation of these issues was treated with a reference simulation of the B-type DNA double helix d(CGCGCGATCGCGCG)$_2$ and a simulation of the DNA with one daunomycin molecule. Also DNA-daunomycin complexes with two daunomycin molecules per oligonucleotide with three different starting conformations were conducted. Each of these simulations was carried out for at least 10 ns with the longest lasting for 20 ns. Another simulation using Locally Enhanced Sampling (LES) was performed for 6 ns, starting from the results showing a high stability of a daunomycin molecule with a distorted glycosidic linkage that was unknown until now and that will be outlined in detail later. It can be easily anticipated that a given canonical B-DNA structure has to undergo structural changes during the process of intercalation. We tried to pin down which changes are predominant and what conformational changes DNA undergoes. Chaires (48) for example found that DNA undergoes a conversion from Z- to B-DNA by intercalation of daunomycin and that B-DNA is stabilized. Especially stacking interactions like the DNA rise and buckle, flexibility of the DNA

Figure 1: Molecular formula of daunomycin displaying the characteristic anthracycline ring system, the cyclohexyl ring and the daunosamine sugar moiety in the protonated ammonium form.
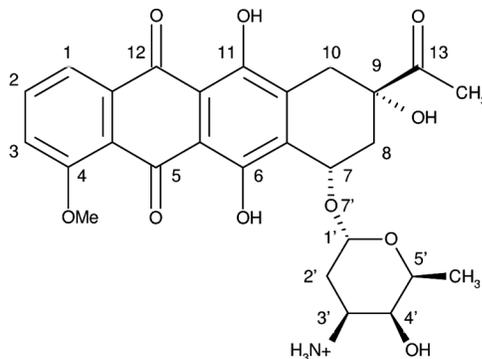
backbone and the groove widths and H-bonding partners in the close vicinity of intercalation responsible for stabilization were investigated. Recently performed investigations showed that B_I/B_{II} transitions occur in the nano- to sub-nanosecond time scale (59, 63). Thus we are able to investigate this behavior in the course of our simulations. The influence of intercalation on the B_I/B_{II} interplay was of major interest. The intercalator-DNA complex is stabilized by stacking of the DNA bases above and below the intercalation site and the aromatic anthracycline ring system. Also hydrogen bonds between the DNA and the positively charged amino-group and the 9-OH group of daunomycin stabilize the complex.

Methods

All simulations were performed using the AMBER6 (64) or AMBER7 (65) package. Standard state of the art simulation protocols were adapted for our needs (59, 60, 66-68). The inclusion of the electrostatical long range interactions via the particle mesh Ewald method (69, 70) allows the accurate calculation of highly charged molecules such as DNA. Thus stable trajectories can be calculated in the nanosecond time range. The DNA structures we found as crystal structures in daunomycin-DNA complexes were hexamers, as mentioned above, and hence too short for our purpose. We constructed a 14-mer of canonical B-DNA (71) using the program NUKIT, that is implemented in AMBER (64), with the sequence d(CGCGCGATCGCGCG)$_2$. We took the structure and coordinates of daunomycin from the X-ray structure determined by Frederick *et al*. (26) (PDB code = 1D10) and performed an ab initio structural minimization and calculation of the electrostatic potential for RESP (Restrained ElectroStatic Potential) (72, 73) with GAUSSIAN98 (74) at the HF/6-31G* level of theory. As our generated DNA did not contain an intercalator molecule, introducing the daunomycin into the DNA was achieved by two different approaches. In the first we positioned the daunomycin molecule by translational movements with the program SYBYL (75) in close vicinity of the intercalation site of the canonical B-DNA and then applied distance restraints of 20 kcal/mol gained from the X-ray structures (the distance restraints used are available as supplementary material). This leads to a geometry of the complex very close to the X-ray structure. The second daunomycin was intercalated into the DNA and added to the first with the same method. But this time the sugar dihedral angle C7-O7-C1′-C2′ of one daunomycin was changed manually to 70º to investigate the conformational flexibility of the sugar residue. In the second approach we used the targeted MD option in AMBER7. For the targeted MD the X-ray structure of Frederick *et al*. (26) was used as the reference structure and the value of the target RMSD was chosen to be 0.0 Å. The force constant was increased stepwise from 5 to 10, 20 and 50 kcal/mol with 10 ps of simulation at each force constant, yielding a final RMSD to the X-ray structure of 0.17 Å. Each strand of the DNA has 13 PO_4^- anions. Daunomycin has one positive charge. In order to achieve electro-neutrality 26 sodium ions were placed around the uncomplexed DNA. For the single and double daunomycin complex 25 and 24 sodium ions were needed, respectively. These ions were positioned using the program Xleap included in the AMBER6 package. Long range interactions are taken into account via the so-called particle mesh Ewald method with a convergence criterion of 0.00001. The temperature is regulated by bath coupling using the Berendsen algorithm (76) and kept at 300 K. General other parameters of the simulation are a time step of 2 fs, constraints of 0.00005 Å for the SHAKE procedure regarding all bonds involving hydrogen atoms and a 9 Å non bonded cutoff. General simulation parameters were kept constant during the whole simulation and the structural information was collected every ps. As force field we used the all atom force field of Cornell *et al*. (77) with the new modifications of Cheatham *et al*. (78). The force field parameters for daunomycin were selected in analogy to existing parameters in the force field. That is the atom types where chosen to meet chemical and structural requirements according to the publication by Cornell *et al*. (77). The angle and dihedral parameters not already present in the parm99 force

field were chosen as outlined in the supplementary materials section and added to the parm99 force field. The resulting model of daunomycin created with Xleap with the assigned atom types and the assigned charges after the RESP procedure are as well available in the supplementary material section. Counterions and water molecules are calculated explicitly using a TIP3P Monte Carlo water box (79) requiring a 12 Å solvent shell in all directions. The minimizations were carried out with harmonic restraints on DNA and counterion positions. These restraints were relaxed stepwise and at the end a 500-step minimization without restraints was performed. A similar procedure was applied for the equilibration. The system was heated from 50 to 300 K during 10 ps under constant-pressure conditions and harmonic restraints. After this procedure the system was switched to constant temperature and pressure. Subsequently the restraints were once again relaxed and finally an unrestrained 5 ps equilibration was carried out. From this point the respective simulations were performed for 10 to 20 ns without the necessity of applying any restraints or constraints onto the DNA or intercalator. Locally Enhanced Sampling (LES) was used for the simulation with two daunomycins per 14-mer of which one has a distorted conformation of the glycosidic linkage. The enhanced sampling is achieved by replacing the sugar ring with five copies of itself, that is, these copies do not interact with each other and they interact with other LES regions and the rest of the system in an average way. By that means the barriers to conformational transitions are reduced as compared to the original system and so it is possible to overcome the energy barriers between the local energy minima more easily. The LES simulation was performed for 6 ns with a time step of 1 fs. The other simulation parameters were as described above.

Analysis tools for the resulting trajectories were carnal and ptraj that are implemented in AMBER6 (64). Other tools used were, RASMOL (80), Molecular Dynamics Toolchest (81) and VMD (82).

Summing up we have performed six different simulations. The first one, denoted further on "1dau", is the single intercalator-DNA complex, the second, "2dau", contains two daunomycins of which one has a distorted sugar dihedral, a LES simulation starting from this one denoted "les2dau". From this LES simulation after 1 ns, showing a relaxed dihedral again a MD was started ("2dau-second"). Starting from a targeted MD referenced to the X-ray structure a third simulation with two intercalators was started ("tgt-2dau"). Finally the DNA 14-mer ("dna") was taken as a reference simulation.

Results

All of our simulations were stable after a maximum time of 350 ps concerning the RMSD calculated in relation to the structures obtained after the minimization and equilibration procedures. That is the RMSD values showed from this time on only fluctuations that are typical for MD simulations and no further drift. Therefore the starting point for our calculations was chosen to be 500 ps. The total and kinetic energies were stable even earlier (results not shown). Hence we obtain our values from a time range of 0.5-10 ns ("1dau", "2dau"), 16 ns ("dna", "tgt-2dau") and 20 ns ("2dau-second") providing us with good statistics. Comparing the structural parameters from the X-ray structure published by Frederick *et al*. (26) with our results we find a good agreement. Also the NMR structural determination of the DNA hexamer sequence d(CGATCG) by Barthwal *et al*. was taken into consideration (83).

We were looking for direct evidence that intercalation changes the B_I/B_{II} population. We expected to find a substantial change in the population as already previously it was found that on stretching of DNA, B_{II} becomes energetically more favorable and more pronounced (84, 85). For that purpose the probability of being in the B_{II} conformation of each phosphate during our simulations was calculated. All time steps in which the phosphate was found to be in B_{II} were summed up,
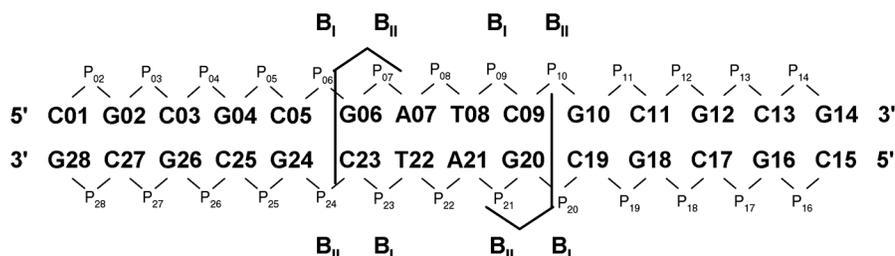
Figure 2: Schematical representation of the DNA indicating the sequence with the two putative intercalation sites at the 5′-CGA-3′ steps and the nomenclature of the backbone phosphates. Daunomycin is represented by an arrow like symbol. Also indicated are the B_I/B_{II} substates of the phosphates around the intercalation sites as described in detail in the text.

divided by the total number of time-steps and compared to uncomplexed DNA. As is evident from Figures 2 and 3 we find a preference of certain phosphates to be in either one of the conformations. These phosphates lie in direct vicinity of the intercalation site. A close up investigation revealed that at each site of intercalation the phosphorus on one strand is in the B_I and the phosphorus directly lying on the opposite strand is in the B_{II} state. This behavior is not subject to fluctuations but stable during all of the simulations. This means that for the double intercalation phosphorus 6 and 20 are in B_I and their corresponding phosphorus 24 and 10 on the opposing strand are in B_{II} almost all of the time. The same is true for single intercalation but only P_{06} and P_{24} are concerned. The adjacent phosphorus atoms downstream behave vice versa: this is for double intercalation P_{07} and P_{21} are in B_{II} whereas P_{09} and P_{23} are in B_I. Again the single intercalation simulation shows similar results with P_{07} in B_{II} and P_{23} in B_I. Our conclusion from this observations is that the intercalation of daunomycin induces and stabilizes a distinct pattern of the phosphates of the DNA backbone. This appears to be a possibility to directly influence the DNA backbone trough complexation and hence leads to a redirection of intercalation caused structural changes to the backbone. These findings have to be compared with the results of Wellenzohn *et al*. (63) and also with the investigations conducted by Kielkopf *et al*. (86) showing that by the complexation of DNA with a polyamide dimer in the minor groove the B_I conformation is dominating at the site of binding. We also found an overall increase of B_{II} when comparing the values for the uncomplexed reference DNA with the systems with one and two daunomycins. That means that the time averaged population of B_{II} rises from 20.2% in the uncomplexed DNA to 26.7% when one daunomycin is intercalated. This increase in B_{II} population is further enhanced to 36.2% when a second intercalator is introduced. That means that two daunomycin molecules effect an almost doubled representation of B_{II} substates compared to uncomplexed DNA. This characteristic can be explained with the already observed fact that DNA stretching is coupled with an increase in B_{II} (59, 87).
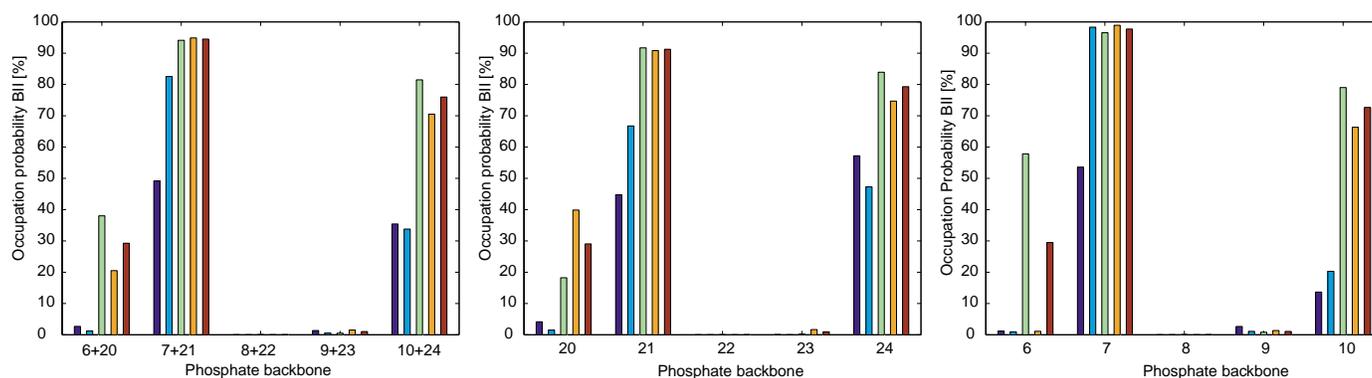
An interesting feature of daunomycin is its sugar ring flexibility, that is pointing into the minor groove and builds stabilizing contacts to the DNA through its charged ammonium group. This sugar also contributes to the sequence specificity and the binding affinity of daunomycin. We compared the dihedral angle formed by the atoms C7-O7-C1′-C2 from five X-ray structures of daunomycin intercalated into DNA of different sequence (protein data bank IDs 110D, 152D, 1D11, 1DA0 and 1JO2) to the X-ray structure we started from (PDB ID 1D10)

Figure 3: The plot on the left shows the occupation probability of phosphates 6 to 10 (see also schematical representation of the DNA backbone and nomenclature in Figure 2), in the center phosphates 20 to 24 and to the right mean values of these phosphates. The color coding is as follows: dark blue "dna", light blue "1dau", green "tgt-2dau", orange "2dau-second" and brown mean value of "tgt-2dau" and "2dau-second". The preference of phosphates 6, 9, 20 and 23 for B_I and of phosphates 7, 10, 21 and 24 for B_{II} with double intercalation is evident.

Trieb et al.
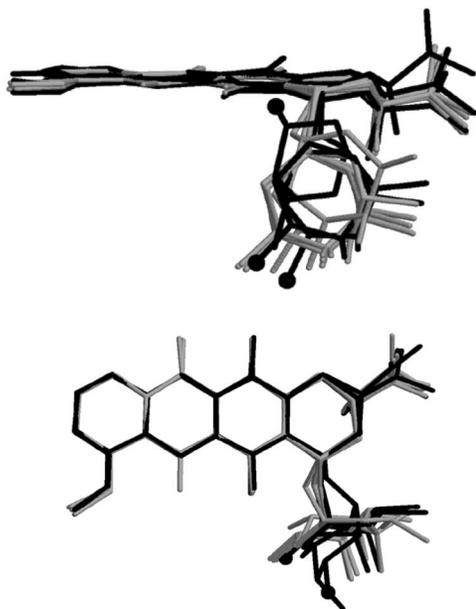
Figure 4: Image of superimposed X-ray crystal structures of daunomycin (PDB IDs 110D, 152D, 1D11, 1DA0, 1JO2 and 1D10) in grey and with the three observed substates of the sugar dihedral found in our simulations in black (position of ammonium group is indicated by a black dot; the dihedral angle decreases clockwise when looking at the dots). Top: view directly onto the sugar ring. Bottom: perpendicular to anthracycline rings.

Figure 5: Plot of the changing sugar dihedral angles of the "2dau-second" simulation during 20 ns. In black and in grey are the two different daunomycins. The three different conformations at around 159, 137 and 59° can clearly be distinguished.
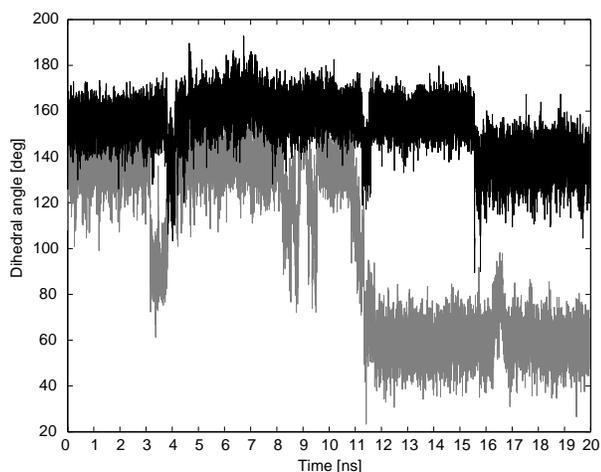
and to our results gained from the simulations. We find that the dihedral angles found in those different X-ray structures vary in the range of 137.1 to 161.6° (see Figure 4).

As mentioned in the methods section one of our simulations with two daunomycins ("2dau") started with a manually distorted sugar dihedral. Due to available X-ray structures and the results of previous structural investigations we see that the daunosamine moiety is quite flexible and thus different conformations of the sugar ring in daunomycin are possible. The glycosidic linkage is flexible and very important for anchoring the intercalator in the minor groove. It appeared to be reasonable to distort the dihedral angle of C7-O7-C1´-C2´ manually from about 145° found in the crystal structure to a value of about 70°. This distortion brings the N3´ ammonium group into different hydrogen bonding distances to hydrogen bond acceptors in the minor groove. To our surprise this conformation was stable after a fast change of the dihedral angle from 70 to 60° for the rest of the 10 ns simulation time. Thus we surmised that we found a stable minimum. To find out, whether this local energetic minimum can be left, we chose two different approaches. In the first we started a LES simulation (as outlined in the methods section) with five copies of the sugar ring and indeed found a fast move of the sugar ring after 400 ps from 60° to 150°. The second daunomycin showed the same angle of 150°. As this angle lies between the other two observed substates of 137 and 159° we surmise that using five copies of the sugar ring in the LES simulation reduced the potential, so that the interchange between these two states is too fast to be distinguished. Another approach to check if the barrier from the 60° dihedral can be overcome was to increase the temperature of the system in our simulation. We started after 5 ns of the regular "2dau" run and increased the temperature to 310 K and simulated for 1 ns – with all other simulation parameters kept constant. Then the temperature was increased to 320 K for 1 ns and finally to 330 K. After about 400 ps at 330 K the dihedral changed spontaneously to 137° and stayed there. No other changes in geometry were observed. That the 60° conformation is also accessible during regular MD runs is proved by the fact that in the "2dau-second" simulation a spontaneous change in the dihedral angle is observed (see Figure 5).

Summing up it can be said that in our simulations we find basically two conformations also represented by X-ray structures but also a third conformation (see Figures 4 and 5). The first one is at 155 to 162°, the second at 135 to 138° and the third shows a dihedral angle value of 57 to 61°.

The interesting thing when looking onto the different conformations of the sugar ring in more detail (Figure 6) is the different way of stabilization through hydrogen bridges. In Figure 6 three snapshots of the trajectory of "2dau-second" are shown. In the 59° conformation we have three hydrogen bonds with heavy atom distances between the nitrogen of the ammonium group and O4´ of guanine (**a**: 3.4 Å) and O5´ of guanine (**b**: 3.0 Å), as well as the distance between the hydroxyl group attached to

the daunosamine moiety and O1P of guanine (**c**: 3.0 Å). Thus three close contacts stabilize this distorted conformation. On the other hand the 137° conformation has an ammonium group to O4´ of cytosine sugar distance of 3.2 Å (**a**) and of 3.0 (**b**) to the O2 atom of thymine. In the 159° conformation, however, these two distances are increased to 5.5 (**a**) and 5.1 Å (**b**), respectively. A hydrogen bonding distance of 3.2 Å is found between the ammonium group and the O4´ of thymine (**c**). Thus the ammonium group of the daunosamine sugar ring that has already been proved to contribute considerably to the binding (12, 88) is differently stabilized in the minor groove and the different positioning and flexibility becomes evident. This stands in good agreement to the findings by Lipscomb *et al*. (89). They compared the displacement factors from X-ray structures of a daunomycin-d(CGATCG)$_2$ complex at room temperature and at -160°. They find higher displacement factors and also thermal mobility for the amino sugar than for the chromophore indicating a variability of the amino sugar. Williams *et al*. (18) studied the complex of 11-deoxydaunomycin with the chemically modified DNA d(CGTsACG) and compared this complex with daunomycin bound to d(CGTACG) and to d(CGATCG). They found a high positional variability of the amino sugar ring in these three different complexes, supporting the hypothesis that the position of the amino sugar is dynamic.
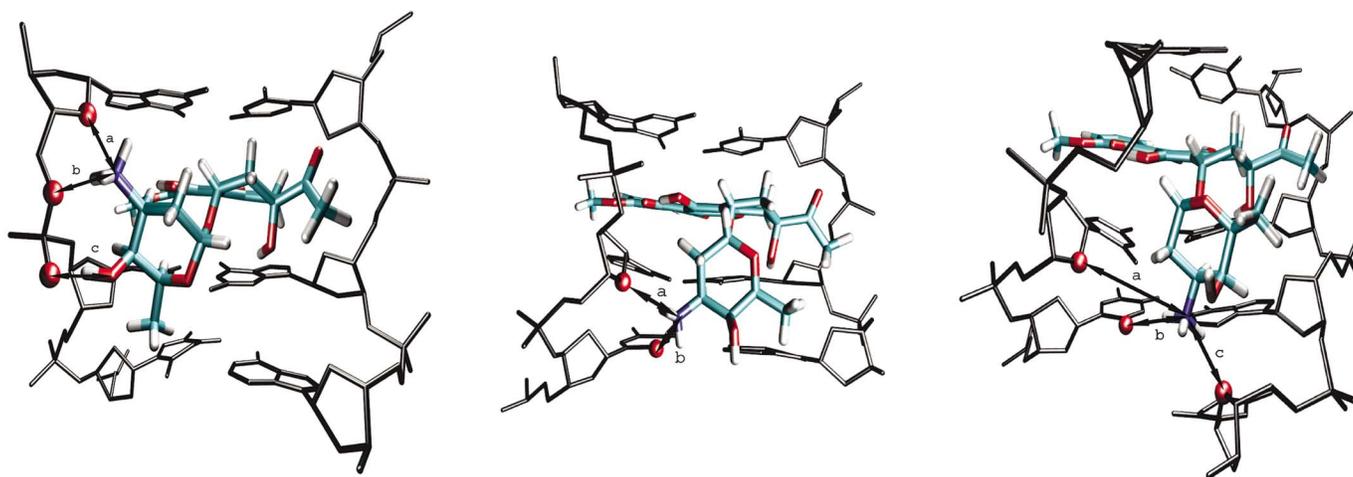
Figure 6: From left to right three snapshots of the trajectory of "2dau-second" are shown which have the three different sugar dihedral conformations of 59, 137 and 159°. For clarity the hydrogen atoms of the DNA are removed. The important distances are indicated by arrows between red circles indicating oxygen atoms and the ammonium group. The numbering is outlined in detail in the text.

From the differences in occupation probability it is possible to calculate the barrier between the conformations. For this purpose we divided the accessible range of dihedral angles into histograms of 1° and summed up the time-steps that lie in each field (Figure 7 shows the resulting graphs). From a logarithmic plot of this probability we can calculate the ΔG‡ values for the barrier between the substates. We find that there is a ΔG‡ of 0.3 to 0.7 kcal/mol between the 159 and the 137° conformations. For the barrier between 137 and 59° we get a value of 1.4 kcal/mol.

As a matter of fact the total length of DNA calculated by adding the rise values gained from dials and windows and skipping the first and the last values due to side effects show that the first daunomycin increases the overall length of the DNA by 3.7 Å and the second by another 3.8 Å. Considering just the step of intercalation an increase of rise of 4.3 Å for each daunomycin compared to uncomplexed DNA is observed (see Figure 8). This corresponds quite well to the increase in rise of 4.1 Å per intercalation site found by Frederick *et al*. (26) and other similar studies (27, 28). This increase in length is exclusively located at the base pairs of intercalation and neither any counter movements are observed in the vicinity nor a transfer of this stretching movement to other base pairs is found.

The buckle parameter is another important feature in intercalation processes as it indicates the movement of the base pairs in the direction of the helix axis. For the mono intercalator complex we observe a buckle of the C5-G24 base pair above the intercalation site of 16.8° and the base pair G6-C23 below -10.7° in the opposite direction (see Figure 10). In the ternary complex the mean values of the three sim-

Figure 7: Plots of the population analysis of the sugar dihedral angle of daunomycin. Black and grey solid lines indicate the two different daunomycin molecules per DNA. Starting on the left upper corner and going clockwise we have the plots of "1dau", "2dau", "tgt-2dau" and "2dau-second". We find the three different conformations accessible during our simulations.

Figure 8: The graph clearly shows the behavior of the rise in the three different systems indicating a high symmetry and an exclusive location at the intercalation sites (uncomplexed DNA with a solid grey line, mono intercalation with a dashed and double intercalation with a solid dark line).

Figure 9: On top the groove width is depicted. It was measured as described in the text (uncomplexed DNA indicated by a grey, single intercalation by a black dashed and double intercalation by a black solid line). We find a substantial widening of the minor groove located almost exclusively at the intercalation sites. At the bottom is a schematical representation of the phosphate backbone represented by circles which was used for the corresponding distances measured for the graph on top. The first value for example is the minor groove width for P_{28}, measured as the normal distance to the line connecting P_{04} and P_{05}.

ulations are comparable (C5-G24: 14.6°, G6-C23: -12.7°, C9-G20: 14.5°, G10-C19: -19.8°). It is interesting to see that the increase in rise alone is not sufficient to accommodate daunomycin and an additional buckle of the concerned base pairs is necessary. The minor groove width was measured by using the perpendicular distance between two adjacent phosphorus atoms on one strand to the most proximate phosphorus on the opposite strand. With this calculation method we get the shortest groove distances and are able to lower the influence that the increase in rise has on the groove widths calculated by other methods. We find a significant widening of the groove at the intercalation sites compared to the reference DNA. Looking at the behavior of DNA we can conclude from the high symmetry of the DNA minor groove that our simulation time is sufficiently long to provide us with good statistics. Intercalation of daunomycin leads to a widening of the minor groove of 2.5 Å for one daunomycin and 1.5 Å for the double intercalation (cf. Figure 9).

This result has to be seen in the context of the unwinding of the DNA which can be estimated by looking at the twist values (90-92). It was previously reported that intercalation leads to an unfolding and unwinding of compact DNA duplexes (91-93). In the X-ray structure we used as a starting point, the twist values don't show a pronounced behavior. Whereas when we compare our results from the uncomplexed DNA reference structure with an averaged twist value of 32.6° (skipping again the terminal values) as seen in the right graph of Figure 10, we are in good agreement with the 36.1° found for 12 different B-DNA structures (94-96). Daunomycin is responsible for a lowering of the twist angle to values of 6.6 degrees for the single intercalation which signifies a quite substantial unwinding of around 26° and is much higher than stated in the complexes investigated for example by X-ray diffraction by Frederick *et al.* (26) and Nunn *et al.* (28). For the double intercalation the change in twist is not that dramatical but still a decrease of 12 to 14 degrees is observed. This unwinding movement can be explained with the necessary rise of the helix axis.

Figure 10: The left graph shows the buckle angles. Uncomplexed DNA is indicated by a green and the X-ray structure by a black solid line, single intercalation is represented by a dashed and double intercalation by a dashed-dotted line. The right graph displays the twist values where the uncomplexed DNA is shown in green, single intercalation is indicated by a solid and double intercalation by a dashed line.
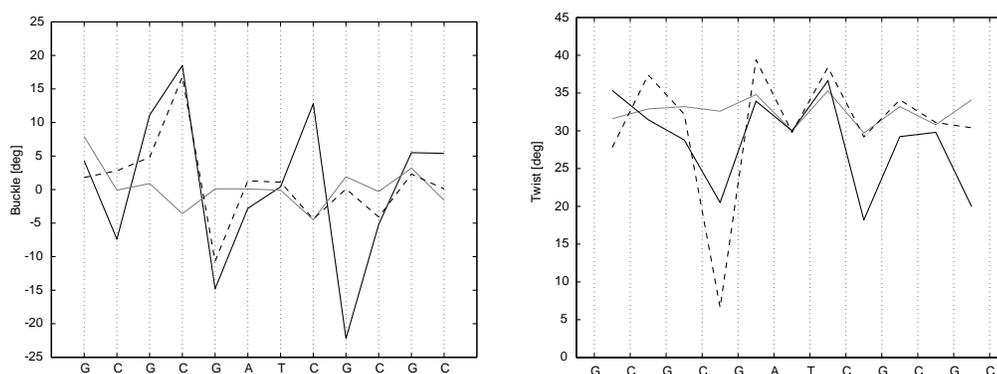
Summary and Conclusion

In the present paper we report several MD simulations of a double stranded 14-mer DNA complexed to the intercalator daunomycin. We took d(CGCGC-GATCGCGCG)$_2$ in the B-form with two putative intercalation sites at the 5´-CGA-3´ step on both strands. With this reference structure we conducted calculations with one and with two intercalating daunomycin molecules. Furthermore, a simulation of a double intercalated DNA with one intercalator showing a distorted amino sugar conformation and a subsequent LES procedure to relax this distortion were made. We find that the daunosamine ring shows a high flexibility in the minor groove fluctuating between three conformational and energetical minima. This allows an adaptation of daunomycin to different environments that are found in different DNA sequences and must be taken into account when evaluating its sequence specificity discussed extensively so far. Of major interest is the fact that the intercalation of daunomycin induces and stabilizes a distinct pattern of B$_I$ and B$_{II}$ around the intercalation site. A conclusion from this is that the changes of DNA geometry caused by intercalation reduce the flexibility of the phosphates and transfers structural information to the backbone. Another important observation is the overall increase in B$_{II}$ that has to be seen in the context of the stretching of the DNA and its unwinding. This once again points out the interconnection between a higher rise and a higher B$_{II}$ population. The comparison of the mono with the double intercalated structure shows a qualitative agreement of the structural data and is consistent with the results obtained by X-ray diffraction with two daunomycins. By providing a longer stretch of DNA and posing the intercalator more centrally we are able to exclude side and crystal packing effects that are inevitable when investigating crystal structures with intercalation sites at terminal base pairs. Regarding the observed rise we can say that the elongation of the DNA is almost exclusively located at the intercalation base steps.

Acknowledgments

References and Footnotes

1. R. B. Weiss. *Sem. Oncol. 19*, 670-686 (1992).
2. F. Barcelo, J. Martorell, F. Gavilanes, J. M. Gonzalez-Ros. *Biochem. Pharm. 37*, 2133-2138 (1988).
3. J. B. Chaires. *Biopolymers 24*, 403-419 (1985).
4. J. B. Chaires, N. Dattagupta, D. M. Crothers. *Biochemistry 24*, 260-267 (1985).
5. P. Cieplak, S. N. Rao, P. D. J. Grootenhuis, P. A. Kollman. *Biopolymers 29*, 717-727 (1990).
6. D. P. Remeta, C. P. Mudd, R. L. Berger, K. J. Breslauer. *Biochemistry 30*, 9799-9809 (1991).
7. J. Ren, T. C. Jenkins, J. B. Chaires. *Biochemistry 39*, 8439-8447 (2000).
8. D. J. Taatjes, G. Gaudanio, K. Resing, T. H. Koch. *J. Med. Chem. 39*, 4135-4138 (1996).
9. X.-L. Yang, A. H.-J. Wang. *Pharmacology and Therapeutics 83*, 181-215 (1999).
10. C. R. Krishnamoorthy, S.-F. Yen, J. C. Smith, J. W. Lown, W. D. Wilson. *Biochemistry 25*, 5933-5940 (1986).
11. F. Frezard, A. Garnier-Suillerot. *Biochimica et Biophysica Acta 1036*, 121-127 (1990).
12. D. J. Cashman, J. N. Scarsdale, G. E. Kellogg. *Nucleic Acids Res. 31*, 4410-4416 (2003).
13. G. R. Clark, P. D. Pytel, C. J. Squire, S. Neidle. *J. Am. Chem. Soc. 125*, 4066-4067 (2003).
14. H. Baruah, U. Bierbach. *Nucleic Acids Res. 31*, 4138-4146 (2003).
15. J. Klass, F. V. Murphy, S. Fouts, M. Serenil, A. Changela, J. Siple, M. E. A. Churchill. *Nucleic Acids Res. 31*, 2852-2864 (2003).
16. S. Jain, M. Polak, N. Hud. *Nucleic Acids Res. 31*, 4608-4615 (2003).
17. H. Robinson, W. Priebe, J. B. Chaires, A. H.-J. Wang. *Biochemistry 36*, 8663-8670 (1997).
18. L. D. Williams, M. Egli, G. Ughetto, G. A. Van der Marel, J. H. Van Boom, G. J. Quigley, A. H.-J. Wang, A. Rich, C. A. Frederick. *J. Mol. Biol. 215*, 313-320 (1990).
19. G. G. Hu, X. Shui, F. Leng, W. Priebe, J. B. Chaires, L. D. Williams. *Biochemistry 36*, 5940-5946 (1997).
20. K.-X. Chen, N. Gresh, B. Pullman, Mol. Pharmacol. 30, 279-286 (1986).
21. Kapur, J. L. Beck, M. M. Sheil. *Rapid Communications in Mass Spectrometry 13*, 2489-2497 (1999).
22. Berger, L. Su, J. R. Spitzner, C. Kang, T. G. Burke, A. Rich. *Nucleic Acids Res. 23*, 4488-4494 (1995).
23. J. B. Chaires, F. Leng, T. Przewloka, I. Fokt, Y.-H. Ling, R. Perez-Soler, W. Priebe. *J. Med. Chem. 40*, 261-266 (1997).
24. H.-J. Wang, G. Ughetto, G. J. Quigley, A. Rich. *Biochemistry 26*, 1152-1163 (1987).
25. H.-J. Wang, Y.-G. Gao, Y.-C. Liaw, Y. Li. *Biochemistry 30*, 3812-3815 (1991).
26. C. A. Frederick, A. H. J. Wang. *Biochemistry 29*, 2538-2549 (1990).
27. M. H. Moore, W. N. Hunter, B. Langlois d'Estaintot. *J. Mol. Biol. 206*, 693-705 (1989).
28. C. M. Nunn, L. Van Meervelt, S. Zhang, M. H. Moore, O. Kenards. *J. Mol. Biol. 222*, 167-177 (1991).
29. G. A. Leonard, T. Brown, W. N. Hunter. *Eur. J. Biochem. 204*, 69-74 (1992).
30. D. B. Davies, R. J. Eaton, S. F. Baranovsky, A. N. Veselkov. *J. Biomol. Struct. Dyn. 17*, 887-901 (2000).
31. X.Qu, J. B. Chaires. *J. Am. Chem. Soc. 123*, 1-7 (2001).
32. M. Feig, B. M. Pettitt. *Biophysical Journal 75*, 134-149 (1998).
33. D. Hamelberg, L. D. Williams, W. D. Wilson. *Nucleic Acids Res. 30*, 3615-3623 (2002).
34. S. Sen, L. Nilsson. *Biophys. J. 77*, 1782-1800 (1999).
35. N. Spackova, I. Berger, M. Egli. *J. Sponer, J. Am. Chem. Soc 120*, 6147-6151 (1998).
36. C. E. Bostock-Smith, S. A. Harris, C. A. Laughton, M. S. Searle. *Nucleic Acids Res. 29*, 693-702 (2001).
37. T. E. Cheatham, M. A. Young. *Biopolymers 56*, 232-256 (2001).
38. M. Karplus. *Acc. Chem. Res. 35*, 321-323 (2002).
39. B. Wellenzohn, W. Flader, R. H. Winger, A. Hallbrucker, E. Mayer, K. R. Liedl. *Nucleic Acids Res. 29*, 5036-5043 (2001).
40. B. Wellenzohn, W. Flader, R. H. Winger, A. Hallbrucker, E. Mayer, K. R. Liedl. *Biochemistry 41*, 4088-4095 (2002).
41. D. Bosch, M. Campillo, L. Pardo. *J. Comput. Chem. 24*, 682-691 (2003).
42. N. Spackova, T. E. Cheatham, F. Ryjacek, F. Lankas, L. van Meervelt, P. Hobza, J. Sponer. *J. Am. Chem. Soc. 125*, 1759-1769 (2003).
43. C. Bailly, G. Chessari, C. Carrasco, A. Joubert, J. Mann, W. D. Wilson, S. Neidle. *Nucleic Acids Res. 31*, 1514-1524 (2003).
44. C. J. Roche, D. Berkowitz, G. A. Sulikowski, S. J. Danishefsky, D. M. Crothers. *Biochemistry 33*, 936-942 (1994).
45. C. J. Roche, J. A. Thomson, D. M. Crothers. *Biochemistry 33*, 926-935 (1994).
46. C. Bailly, D. Suh, M. J. Waring, J. B. Chaires. *Biochemistry 37*, 1033-1045 (1998).
47. G. E. Kellogg, J. N. Scarsdale, F A. Fornari. *Nucleic Acids Res. 26*, 4721-4732 (1998).

48. J. B. Chaires. *Biochemistry 24*, 7479-7486 (1985).

49. G. Gupta, M. Bansal, V. Sasiskharan. *Proc. Natl. Acad. Sci. USA 77*, 6486-6490 (1980).

50. V. Fratini, M. L. Kopka, H. R. Drew, R. E. Dickerson. *J. Biol. Chem. 257*, 14686-14707 (1982).

51. G. G. Privé, U. Heinemann, S. Chandrasegaran, L.-S. Kan, M. L. Kopka, R. E. Dickerson. *Science 238*, 498-504 (1987).

52. B. Schneider, S. Neidle, H. M. Berman. *Biopolymers 42*, 113-124 (1997).

53. W. B. T. Cruse, S. A. Salisbury, T. Brown, R. Cosstick, F. Eckstein, O. Kennard. *J. Mol. Biol. 192*, 891-905 (1986).

54. H. Shindo, T. Fujiwara, H. Akutsu, U. Masumoto, M. Shimidzu. *J. Mol. Biol. 174*, 221-229 (1984).

55. V. Sklenar, A. Bax. *J. Am. Chem. Soc. 109*, 7525-7526 (1987).

56. D. G. Gorenstein. *Chemical Reviews 94*, 1315-1338 (1994).

57. S. Rüdisser, A. Hallbrucker, E. Mayer. *J. Am. Chem. Soc. 119*, 12251-12256 (1997).

58. H. O. Bertrand, T. Ha-Duong, S. Fermandjian, B. Hartmann. *Nucleic Acids Res. 26*, 1261-1267 (1998).

59. R. H. Winger, K. R. Liedl, S. Rüdisser, A. Pichler, A. Hallbrucker, E. Mayer. *J. Phys. Chem. B 102*, 8934-8940(1998).

60. M. A. Young, G. Ravishanker, D. L. Beveridge. *Biophysical Journal 73*, 2313-2336 (1997).

61. T. E. Cheatham, P. A. Kollman. *J. Am. Chem. Soc. 119*, 4805-4825 (1997).

62. Pichler, S. Rüdisser, M. Mitterböck, C. G. Huber, R. H. Winger, K. R. Liedl, A. Hallbrucker, E. Mayer. *Biophysical Journal 77*, 398-409 (1999).

63 B. Wellenzohn, W. Flader, R. H. Winger, A. Hallbrucker, E. Mayer, K. R. Liedl. *J. Am. Chem. Soc. 123*, 5044-5049 (2001).

64. D. A. Case, D. A. Pearlman, J. W Caldwell., T. E. Cheatham, W. S. Ross, C. L. Simmerling, T. A. Darden, K. M. Merz, R. V. Stanton, A. L. Cheng, J. J. Vincent, M. Crowley, V. Tsui, R. J. Radmer, Y. Duan, J. Pitera, I. Massova, G. L. Seibel, U. C. Singh, P. K. Weiner, P. A. Kollman. *University of California San Francisco* (1999).

65. D. A. Case, D. A. Pearlman, J. W. Caldwell, T. E. Cheatham, J. Wang, W. S. Ross, C. L. Simmerling, T. A. Darden, K. M. Merz, R. V. Stanton, A. L. Cheng, J. J. Vincent, M. Crowley, V. Tsui, H. Gohlke, R. J. Radmer, Y. Duan, J. Pitera, I. Massova, G. L. Seibel, U. C. Singh, P.K. Weiner, P. A. Kollman. *University of California San Francisco* (2002).

66. M. A. Young, B. Jayaram, D. L. Beveridge. *J. Am. Chem. Soc. 119*, 59-69 (1997).

67. O. N. de Souza, R. L. Ornstein. *Biophysical Journal 72*, 2395-2397 (1997).

68. O. N. de Souza, R. L. Ornstein. *J. Biomol. Struct. Dyn. 14*, 607-611 (1997).

69. D. M. York, A. Wlodawer, L. G. Pedersen, T. A. Darden. *Proc. Natl. Acad. Sci. USA 91*, 8715-8718 (1994).

70. T. E. Cheatham, P. A. Kollman. *J. Mol. Biol. 259*, 434-444 (1996).

71. S. Arnott, P. J. Campbell-Smith, R. Chandrasekaran. *CRC Handbook of Biochemistry and Molecular Biology*, CRC Press Boca Raton (1976).

72. C. I. Bayly, P. Cieplak, W. D. Cornell, P. A. Kollman. *Journal of Physical Chemistry 97*, 10269-10280 (1993).

73. J. Wang, P. Cieplak, P. A. Kollman. *J. Comput. Chem. 21*, 1049-1074 (2000).

74. M. J. Frisch, G. W. Trucks, H. B. Schlegel, G. E. Scuseria, M. A. Robb, J. R. Cheeseman, V. G. Zakrzewski, J. A. Montgomery, R. E. Stratmann, J. C. Burant, S. Dapprich, J. M. Milliam, A. D. Daniels, Kudin K. N., M. C.Strain, O. Farkas, J. Tomasi, G. A. Petersson, P. Y. Ayala, Q. Cui, K. Morokuma, D. K. Malick, A. D. Rabuck, K. Raghvachari, J. B. Foresman, J. Cioslowski, J. V. Ortiz, B. B. Stefanov, G. Liu, A. Liashenko, P. Piskorz, I. Komaromi, R. Gomperts, R. L. Martin, D. J. Fox, T. Keith, M. A. Al-Laham, C. Y. Peng, A. Nanayakkara, C. Gonzalez, M. Challacombe, P. M. W. Gill, B. G. Johnson, W. Chen, M. W. Wong, J. L. Andres, M. Head-Gordon, E. S. Replogle, J. A. Pople. *Gaussian98* (Revision A.1), Gaussian Inc. Pittsburgh PA (1995).

75. SYBYL 6.6, Tripos Inc. 1699 South Hanley Road St. Louis Missouri 63144 USA.

76. H. J. C. Berendsen, J. P. M. Postma, W. F. Van Gunsteren, A. DiNola, J. R. Haak. *Journal of Chemical Physics 81*, 3684-3690 (1984).

77. W. D. Cornell, P. Cieplak, C. I. Bayly, I. R. Gould, K. M. Merz, D. M. Ferguson, D. C. Spellmeyer, T. Fox, J. W. Caldwell, P. A. Kollman. *J. Am. Chem. Soc. 117*, 5179-5197 (1995).

78. T. E. Cheatham, P. Cieplak, P. A. Kollman. *J. Biomol. Struct. Dyn. 16*, 845-862 (1999).

79. W. L. Jorgensen. *J. Am. Chem. Soc. 103*, 335-340 (1981).

80. R. Sayle, *RasMol 2.6.*, Glaxo Wellcome Medicines Research Centre Hertfordshire UK (1995).

81. G. Ravishanker, S. Swaminathan, D. L. Beveridge, R. Lavery, H. Sklenar. *J. Biomol. Struct. Dyn. 6*, 669-699 (1989).

82. P. Grayson, J. Gullingsrud, B. Isralewitz, D. Norris, J. Stone. *VMD User's Guide. Theoretical Biophysics Group University of Illinois and Beckman Institute*. Version 1.7.1 edition (2001).

83. R. Barthwal, Monica, P. Awasthi, N. Srivastava, U. Sharma, M. Kaur, G. Govil. *J. Biomol. Struct. Dyn. 21*, 407-423 (2003).

84. K. M. Kosikov, A. A. Gorin, V. B. Zhurkin, W. K. Olson. *J. Mol. Biol. 289*, 1301-1326 (1999).

85. G. Bertucat, R. Lavery, C. Prevost. *J. Biomol. Struct. Dyn. 16*, 535-546 (1998).

86. C. L. Kielkopf, S. Ding, P. Kuhn, D. C. Rees. *J. Mol. Biol. 296*, 787-801 (2000).

87. K. Grzeskowiak, K. Yanagi, G. G. Privé, R. E. Dickerson. *J. Biol. Chem. 266*, 8861-8883 (1991).

88. J. B. Chaires, S. Satyanarayana, D. Suh, I. Fokt, T. Przewolka, W. Priebe. *Biochemistry 35*, 2047-2053 (1996).

89. L. A. Lipscomb, M. E. Peek, F. X. Zhou, J. A. Bertrand, D. VanDerveer, L. D. Williams. *Biochemistry 33*, 3649-3659 (1994).

90. C. Medhi, J. B. O. Mitchell, S. L. Price, A. B. Tabor. *Biopolymers 52*, 84-93 (1999).

91. F. A. Fornari, J. K. Randolph, J. C. Yalowich, M. K. Ritke, D. A. Gerwitz. *Mol. Pharmacol 45*, 649-656 (1994).

92. S. M. Zeman, K. M. Depew, S. J. Danishefsky, D. M. Crothers. *Proc. Natl. Acad. Sci. USA 95*, 4327-4332 (1998).

93. Y. Yoshikawa, K. Yoshikawa, T. Kanbe. *Biophysical Chemistry 61*, 93-100 (1996).

94. V. A. Bloomfield, D. M. Crothers, I. Jr. Tinoco. *Nucleic Acids: Structures Properties and Functions*. University Science Books (1999).

95. R. E. Dickerson. *Methods Enzymol. 211*, 67-111 (1992).

96. K. Yanagi, G. G. Privé, R. E. Dickerson. *J. Mol. Biol. 217*, 201-214 (1991).